Parametrization of general seismic potency and moment tensors for source inversion of seismic waveform data

Lupei Zhu[1] and Yehuda Ben-Zion[2]

[1]*Department of Earth and Atmospheric Sciences, Saint Louis University, St. Louis, MO 63103, USA. E-mail: zhul@slu.edu*
[2]*Department of Earth Sciences, University of Southern California, Los Angeles, CA 90089, USA*

SUMMARY

We decompose a general seismic potency tensor into isotropic tensor, double-couple tensor and compensated linear vector dipole using the eigenvectors and eigenvalues of the full tensor. Two dimensionless parameters are used to quantify the size of the isotropic and compensated linear vector dipole components. The parameters have well-defined finite ranges and are suited for non-linear inversions of source tensors from seismic waveform data. The decomposition and parametrization for the potency tensor are used to obtain corresponding results for a general seismic moment tensor. The relations between different parameters of the potency and moment tensors in isotropic media are derived. We also discuss appropriate specification of the relative size of different source components in inversions of seismic data.

Key words: Earthquake dynamics; Earthquake source observations; Theoretical seismology; Dynamics and mechanics of faulting.

1 INTRODUCTION

A seismic source inside a body with zero net force and torque is represented mathematically by a 3×3 symmetric tensor with six independent components (e.g. Aki & Richards 2002). The ground motion generated by seismic sources can be expressed as a linear combination of the relevant elastodynamic Green's functions with coefficients given by the six components of the source tensor. If the hypocenter and velocity structure between the source and stations are known, the source tensor can be determined from observed seismograms. The most commonly used specification of seismic sources is the moment tensor defined as the integral of the 'stress glut' over the source volume (e.g. Dahlen & Tromp 1998). Alternatively, seismic sources may be specified using the potency tensor defined as the integral of the 'transformational strain' over the source volume (e.g. Ben-Zion 2003). The source tensor provides fundamental information on the event magnitude, source geometry (e.g. possible fault plane orientations and slip directions), and partitioning among various deviatoric and isotropic components. Ben-Zion (2001) noted that it is better to use the strain-based potency tensor than the stress-based moment, since the potency involves only directly observable quantities whereas the moment requires making assumptions on elastic properties at the source. This can be important since the elastic moduli vary rapidly (and elasticity breaks down) in the space–time windows associated with seismic sources. See also Ben-Zion (1989), Heaton & Heaton (1989), Ampuero & Dahlen (2005), Ben-Zion (2008), Chapman & Leaney (2012).

The moment tensors of global earthquakes with magnitudes larger than 5 are routinely determined using broad-band waveform data (Ekstrom *et al.* 2012). In regions where dense seismic networks operate, the magnitude thresholds can be lowered down to 4 (e.g. Dreger & Helmberger 1993; Ritsema & Lay 1993; Zhu & Helmberger 1996; Pondrelli *et al.* 2006). Most of the moment–tensor derivations use a linear inversion to determine the six tensor components directly. However, event mislocation and imperfect velocity models can make the linear inversion less reliable, especially when high-frequency waveform data are used for moderate-to-small-sized events. Zhao & Helmberger (1994) and Zhu & Helmberger (1996) developed the Cut-and-Paste (CAP) method to account for event mislocation and imperfect Green's functions. The CAP method breaks the seismograms into *P*- and *S*-wave segments and allows time-shifts between the observed and predicted waveforms. The added unknown parameters of the time-shifts turn the source tensor determination into a non-linear inverse problem, for which global optimization methods such as grid search, the neighborhood algorithm, and simulated annealing are often used. Solving the inverse problem requires specifying the source tensor by a set of six different parameters with known and finite possible value ranges. The original CAP method limits the seismic sources to be a pure double couple, which reduces the unknown tensor parameters to four, and uses a grid search to find the best moment magnitude, strike and dip of the fault plane and slip direction.

Although most tectonic earthquakes are dominated by shear deformation in a narrow zone, non-double couple seismic sources have been observed in volcanic and geothermal regions (e.g. Julian & Sipkin 1985; Foulger *et al.* 2004; Minson *et al.* 2007), and for other natural or man-made seismic events such as mine collapses and nuclear explosions (e.g. Dreger & Woods 2002; Walter *et al.* 2009;

Patton & Taylor 2011). Recently, Ben-Zion & Ampuero (2009) derived a seismic representation theorem that includes a 'damage-related' radiation produced by coseismic changes of elastic moduli in the source volume. Order of magnitude estimates indicate that the damage-related contribution to motion in the bulk can have appreciable amplitude. A decomposition analysis shows that the damage-related source term can have a significant isotropic component. Motivated by these theoretical results, we update the source specification in the original CAP method to include non-double couple components in the inversion. In the following sections we present a compact parametrization of general seismic source tensors that will be used in a generalized CAP (gCAP) method.

We start with the more elementary potency tensor and decompose it into isotropic (ISO), double-couple (DC) and compensated linear vector dipole (CLVD) source terms using the eigenvectors and eigenvalues of the tensor. This eigenvector-based approach was used by others to decompose a general moment tensor (e.g. Hudson *et al.* 1989; Jost & Herrmann 1989; Riedesel & Jordan 1989; Tape & Tape 2012a). The obtained isotropic tensor is unique, but the decomposition of the remaining deviatoric tensor into DC and CLVD terms is not. Consequently, as reviewed by Julian *et al.* (1998) and Chapman & Leaney (2012), there are several DC–CLVD decompositions in the literature. We use the one recommended by Chapman & Leaney (2012) where the CLVD is orthogonal to the DC tensor, which enables a convenient separation of the contributions and errors of these two source terms. We introduce two dimensionless parameters with finite ranges of values to quantify the size of the ISO and CLVD components. This provides a suitable parametrization for non-linear inversions of seismic source tensors. A general seismic moment tensor is decomposed and parametrized in parallel to what is done for the potency. The relations between parameters of the potency and moment tensors in isotropic elasticity, and appropriate size specification of different source components, are derived and discussed.

2 SEISMIC POTENCY TENSOR

Following standard practice, a general seismic potency tensor is decomposed into isotropic and deviatoric components

$$P_{ij} = \frac{1}{3} tr(\mathbf{P})\delta_{ij} + P'_{ij}. \tag{1}$$

We introduce a dimensionless parameter ζ to quantify the strength of the isotropic potency term

$$\zeta = \sqrt{\frac{2}{3}} \frac{tr(\mathbf{P})}{P_0}, \tag{2}$$

where

$$P_0 \equiv \sqrt{2P_{ij}P_{ij}}, \tag{3}$$

is the scalar potency (e.g. Ben-Zion 2003). It can be shown that ζ varies from -1 (implosion) to 1 (explosion).

Using the scalar parameters P_0 and ζ, (1) can be written as

$$P_{ij} = \frac{P_0}{\sqrt{2}} \left(\zeta I_{ij} + \sqrt{1 - \zeta^2} D_{ij} \right), \tag{4}$$

with normalized isotropic tensor

$$I_{ij} = \frac{1}{\sqrt{3}} \delta_{ij}, \tag{5}$$

and normalized deviatoric tensor D_{ij} satisfying

$$D_{ii} = 0, \tag{6}$$

$$D_{ij}D_{ij} = 1. \tag{7}$$

Next we decompose D_{ij} into double-couple and CLVD components. The CLVD has a dipole of magnitude 2 in its symmetry axis compensated by two unit dipoles in the orthogonal directions (Knopoff & Randall 1970). Let λ_1 be the largest eigenvalue (corresponding to the *T*-axis eigenvector $\hat{T}$) of the deviatoric tensor D_{ij}, λ_2 be the intermediate eigenvalue (corresponding to the null-axis eigenvector $\hat{N}$), and λ_3 the smallest eigenvalue (corresponding to the *P*-axis eigenvector $\hat{P}$), that is,

$$\lambda_1 \geq \lambda_2 \geq \lambda_3. \tag{8}$$

This follows the convention that extension and compression are positive and negative, respectively. Note that all λ_i's are dimensionless. Eqs (6) and (7) imply that the eigenvalues satisfy the conditions

$$\lambda_1 + \lambda_2 + \lambda_3 = 0, \tag{9}$$

$$\lambda_1^2 + \lambda_2^2 + \lambda_3^2 = 1. \tag{10}$$

Using (8)–(10), we get

$$\max(\lambda_2) = \min(\lambda_1) = \frac{1}{\sqrt{6}}, \tag{11}$$

$$\min(\lambda_2) = \max(\lambda_3) = -\frac{1}{\sqrt{6}}. \tag{12}$$

When $\lambda_2 = 0$, the deviatoric tensor D_{ij} is a pure double-couple.

As mentioned, the DC–CLVD decomposition is not unique as the CLVD symmetry axis can be aligned with any of the principal axes (e.g. Hudson *et al.* 1989; Jost & Herrmann 1989). Here we align the CLVD symmetry axis with the *N*-axis (e.g. Chapman & Leaney 2012)

$$D_{ij} = \lambda_1 T_i T_j + \lambda_2 N_i N_j + \lambda_3 P_i P_j$$

$$= \frac{\lambda_1 - \lambda_3}{\sqrt{2}} D_{ij}^{\text{DC}} + \sqrt{\frac{3}{2}} \lambda_2 D_{ij}^{\text{CLVD}}, \tag{13}$$

where

$$D_{ij}^{\text{DC}} = \frac{1}{\sqrt{2}} (T_i T_j - P_i P_j), \tag{14}$$

$$D_{ij}^{\text{CLVD}} = \frac{1}{\sqrt{6}} (2N_i N_j - T_i T_j - P_i P_j), \tag{15}$$

are normalized DC and CLVD tensors. The above decomposition has the attractive property that the DC and CLVD basic sources are orthogonal

$$D_{ij}^{\text{DC}} D_{ij}^{\text{CLVD}} = 0. \tag{16}$$

The strength of the CLVD component can be quantified by the dimensionless parameter

$$\chi = \sqrt{\frac{3}{2}} \lambda_2. \tag{17}$$

It can be shown from (11) and (12) that $0.5 \geq \chi \geq -0.5$. Bailey *et al.* (2009) used the same parameter to quantify the CLVD component in analysis of summed earthquake potency tensors, and compared it (their fig. C1) to other measures of the strength of the CLVD term. See also Julian *et al.* (1998).

Using (7) and (17), Eq. (13) can now be written as

$$D_{ij} = \sqrt{1 - \chi^2} D_{ij}^{\text{DC}} + \chi D_{ij}^{\text{CLVD}}. \tag{18}$$

Inserting (18) into (4), we express a general potency tensor as

$$P_{ij} = \frac{P_0}{\sqrt{2}}\left(\zeta I_{ij} + \sqrt{1-\zeta^2}\left(\sqrt{1-\chi^2}D_{ij}^{\mathrm{DC}} + \chi D_{ij}^{\mathrm{CLVD}}\right)\right). \quad (19)$$

As seen, a full specification of the potency tensor involves six independent parameters: three amplitude factors P_0, ζ and χ, and three angles determining the orientations of the principal axes of the deviatoric tensor (e.g. a fault-based coordinate system with strike ϕ, dip δ and slip angle on the fault λ, see Aki & Richards 2002, pages 108–109).

3 SEISMIC MOMENT TENSOR

Following similar procedures, we can express a general seismic moment tensor as

$$M_{ij} = \sqrt{2}M_0\left(\zeta_m I_{ij} + \sqrt{1-\zeta_m^2}D_{ij}'\right). \quad (20)$$

Here M_0 is the scalar moment defined as

$$M_0 \equiv \sqrt{\frac{M_{ij}M_{ij}}{2}}, \quad (21)$$

and ζ_m is a dimensionless parameter quantifying the strength of the isotropic moment,

$$\zeta_m = \frac{tr(\mathbf{M})}{\sqrt{6}M_0}, \quad (22)$$

with $1 \geq \zeta_m \geq -1$. The normalized deviatoric moment tensor D_{ij}' is expressed in the same form as in (18) but using its own eigenvalues and principal axes. Therefore, a general moment tensor can also be described using six independent parameters: M_0, ζ_m, χ_m, ϕ_m, δ_m and λ_m. The subscript m emphasizes that these parameters, although similar, are in general not the same as those for the potency tensor. The moment tensor is linearly related to the potency tensor through the fourth-order elastic moduli tensor (e.g. Ben-Zion 2003),

$$M_{ij} = c_{ijkl}P_{kl}. \quad (23)$$

For isotropic elastic media,

$$M_{ij} = \left(\lambda + \frac{2}{3}\mu\right)P_{kk}\delta_{ij} + 2\mu P_{ij}', \quad (24)$$

where λ and μ are the Lame constants. Using (4) this becomes

$$M_{ij} = \sqrt{2}\mu P_0\left(\eta\zeta I_{ij} + \sqrt{1-\zeta^2}D_{ij}\right), \quad (25)$$

where $\eta = \frac{1+\nu}{1-2\nu}$ and ν is the Poisson's ratio. Comparing (20) and (25) it is seen that for isotropic elasticity,

$$D_{ij}' = D_{ij}. \quad (26)$$

This indicates that in isotropic solids the CLVD parameters and source orientation angles for the moment and potency tensors are the same

$$\chi_m = \chi, \quad \phi_m = \phi, \quad \delta_m = \delta, \quad \lambda_m = \lambda. \quad (27)$$

However, the isotropic moment parameter is related to the isotropic potency parameter as

$$\zeta_m = \frac{\eta\zeta}{\sqrt{1-(1-\eta^2)\zeta^2}}. \quad (28)$$

Furthermore, the scalar moment is related to the scalar potency by

$$M_0 = \mu P_0\sqrt{1-(1-\eta^2)\zeta^2}. \quad (29)$$

For sources without volumetric change ($\zeta = 0$), (29) reduces to the commonly-used relationship

$$M_0 = \mu P_0. \quad (30)$$

Fig. 1 illustrates the variations of ζ_m and M_0 over μP_0 versus ζ for different Poisson's ratios.

4 DISCUSSION

Hudson *et al.* (1989) introduced two dimensionless parameters k and T to represent, respectively, the isotropic and CLVD components of a moment tensor, using the trace of the moment tensor and the intermediate eigenvalue of the deviatoric tensor. Our dimensionless parameters ζ_m and χ_m correspond, respectively, to k and T. However, the scaling factor of k and T is the trace plus the maximum eigenvalue magnitude of the deviatoric tensor, while our parameters in (2) and (17) are scaled directly by the size of the seismic event given by the scalar potency P_0 or scalar moment M_0. The Hudson *et al.* (1989) parameters provide useful graphical display of different source types of moment tensor inversion results. However, due to the lack of the scalar moment in that parameterization, and the
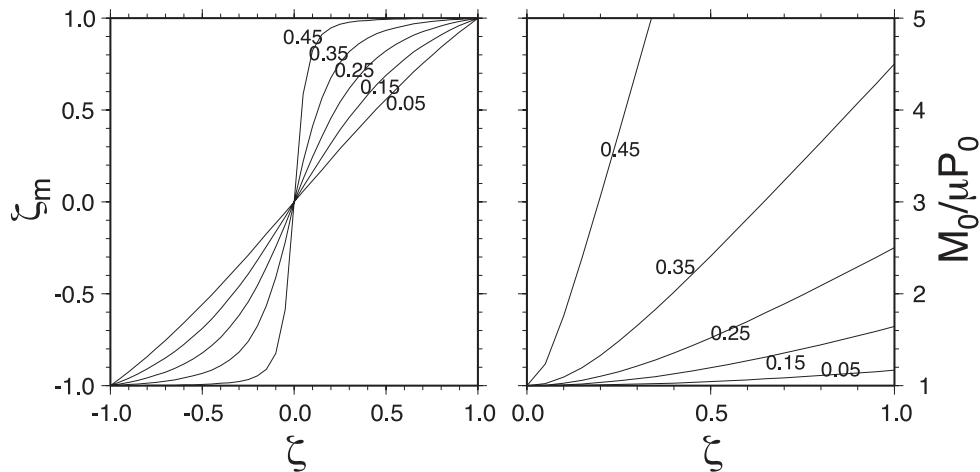
Figure 1. Variations of the isotropic moment parameter ζ_m (left) and the ratio of scalar moment over scalar potency times rigidity (right) versus the isotropic potency parameter ζ for different Poisson's ratios.

dependence of the CLVD alignment on the sign of the intermediate eigenvalue, they are not suitable for moment tensor inversions, as the expression of a general moment tensor in terms of these parameters is cumbersome.

Tape & Tape (2012a,b) recently described a parametrization for use in moment tensor inversion and display. The source type is specified by two angular parameters: colatitude β and longitude γ on a section (or lune with $\pi/6 \geq \gamma \geq -\pi/6$) of the focal sphere. See also Riedesel & Jordan (1989). Isotropic sources are located at the north and south poles and pure DC sources are located at the centre of the lune on the equator. Since we use the same tensor decomposition as in Riedesel & Jordan (1989) and Tape & Tape (2012a), our dimensionless parameters ζ_m and χ_m are directly related to β and γ. Comparing our (17) and (22) with (21ab) of Tape & Tape (2012a) gives

$$\zeta_m = \cos\beta, \tag{31}$$

$$\chi_m = \sin\gamma. \tag{32}$$

The two sets of parameterization are equivalent and somewhat complementary. The angular parameters are geometrical in nature and highly suitable for graphic display of different types of source tensors. On the other hand, our parameters ζ_m and χ_m emphasize the physical properties of isotropic source component (using the ratio of pressure and M_0) and CLVD component (using the ratio of the intermediate eigenvalue and the norm of the deviatoric moment tensor).

There have been some confusions in the literature on quantifying the relative strengths of different components of a seismic source tensor. The Hudson parameters k and $\tau = (1 - |k|)T$ were often used to represent the percentages of isotropic and CLVD components. This is incorrect due to lack of normalization of their basic source tensors (e.g. Chapman & Leaney 2012). We emphasize that our isotropic parameter ζ can represent the fractional volumetric source component, but the CLVD parameter χ is only the relative strength of the CLVD component within the deviatoric tensor. Following Chapman & Leaney (2012), we suggest using squared ratios of the scalar potency of each component to the total scalar potency to represent the relative strengths of the ISO, DC, and CLVD components in a general seismic source

$$\Lambda^{ISO} = \text{sgn}(\zeta)\zeta^2, \tag{33}$$

$$\Lambda^{DC} = (1 - \zeta^2)(1 - \chi^2), \tag{34}$$

$$\Lambda^{CLVD} = \text{sgn}(\chi)(1 - \zeta^2)\chi^2, \tag{35}$$

such that

$$|\Lambda^{ISO}| + \Lambda^{DC} + |\Lambda^{CLVD}| = 1. \tag{36}$$

The permissible values of different fractional strengths are shown in Fig. 2. The graph is similar to the τ–k diamond plot of Hudson *et al.* (1989) and the lune display of Tape & Tape (2012a). Note that the maximum CLVD strength in this decomposition is 25 per cent (at $\zeta = 0$ and $\chi = \pm 1/2$).

In conclusion, we present basic parametrization of general seismic potency and moment tensors amenable for practical inversions of source properties from recorded seismograms. We clarify the relations between parameters of the potency and moment tensors in isotropic elastic solids, and provide guidelines on specifying the relative strength of the ISO, DC and CLVD source terms in our and other representations. The developed parametrization has been
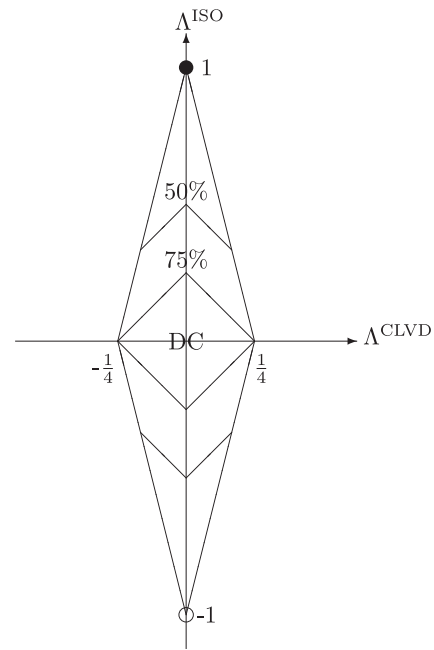
Figure 2. Diagram showing permissible values of the fractional source strengths Λ^{ISO}, Λ^{CLVD} and Λ^{DC} bounded by the outer diamond. The pure explosion and implosion sources are indicated by the solid and open circles, respectively. The pure DC source is located at the center. The contours show DC levels of 75 and 50 per cent.

implemented in a generalized version of the CAP inversion that is hereafter referred to as the gCAP method. Results on observed earthquake source tensor properties based on the gCAP method will be presented in a follow-up paper.

ACKNOWLEDGEMENTS

REFERENCES

Aki, K. & Richards, P.G., 2002. *Quantitative Seismology,* 2nd edn. University Science Books, Sausalito, CA.

Ampuero, J.-P. & Dahlen, F.A., 2005. Ambiguity of the moment tensor, *Bull. seism. Soc. Am.,* **95,** 390–400.

Bailey, I.W., Becker, T.W. & Ben-Zion, Y., 2009. Patterns of co-seismic strain computed from southern California focal mechanisms, *Geophys. J. Int.,* **177,** 1015–1036.

Ben-Zion, Y., 1989. The response of two joined quarter spaces to SH line sources located at the material discontinuity interface, *Geophys. J. Int.,* **98,** 213–222.

Ben-Zion, Y., 2001. On quantification of the earthquake source, *Seism. Res. Lett.,* **72,** 151–152.

Ben-Zion, Y., 2003. Key formulas in earthquake seismology, in *International Handbook of Earthquake and Engineering Seismology,* pp. 1857–1875, ed. Lee, W.H.K. & Part, B., Academic Press, Boston, MA, USA.

Ben-Zion, Y., 2008. Collective behavior of earthquakes and faults: continuum-discrete transitions, progressive evolutionary changes and different dynamics regimes, *Rev. Geophys.,* **46,** RG4006, doi:10.1029/2008RG000260.

Ben-Zion, Y. & Ampuero, J., 2009. Seismic radiation from regions sustaining material damage, *Geophys. J. Int.,* **178,** 1351–1356.

Chapman, C.H. & Leaney, W.S., 2012. A new moment-tensor decomposition for seismic events in anisotopic media, *Geophys. J. Int.,* **188,** 343–370.

Dahlen, F.A. & Tromp, J., 1998. *Theoretical Global Seismology,* Princeton University Press, Princeton, NJ.

Dreger, D. & Woods, B., 2002. Regional distance seismic moment tensors of nuclear explosions, *Tectonophysics,* **356,** 139–156.

Dreger, D.S. & Helmberger, D.V., 1993. Determination of source parameters at regional distances with three-component sparse network data, *J. geophys. Res.,* **98,** 8107–8125.

Ekstrom, G., Nettles, M. & Dziewonski, A.M., 2012. The global CMT project 2004–2010: centroid-moment tensor for 13,017 earthquakes, *Phys. Earth planet. Inter.,* **200–201,** 1–9.

Foulger, G.R., Julian, B.R., Hill, D.P., Pitt, A.M., Malin, P.E. & Shalev, E., 2004. Non-double-couple microearthquakes at Long Valley Caldera, California, provide evidence for hydraulic fracturing, *J. Volc. Geotherm. Res.,* **132,** 45–71.

Heaton, T.H. & Heaton, R.E., 1989. Static deformation from point forces and force couples located in welded elastic Poissonian half-spaces: implications for seismic moment tensors, *Bull. seism. Soc. Am.,* **79,** 813–841.

Hudson, J.A., Pearce, R.G. & Rogers, R.M., 1989. Source type plot for inversion of the moment tensor, *J. geophys. Res.,* **94,** 765–774.

Jost, M.L. & Herrmann, R.B., 1989. A student's guide to and review of moment tensors, *Seismol. Res. Lett.,* **60,** 37–57.

Julian, B.R. & Sipkin, S.A., 1985. Earthquake processes in the Long Valley Caldera area, California, *J. geophys. Res.,* **90,** 11 155–11 169.

Julian, B.R., Miller, A.D. & Foulger, G.R., 1998. Non-double-couple earthquakes: 1. theory, *Rev. Geophys.,* **36,** 525–549.

Knopoff, L. & Randall, M.J., The compensated linear-vector dipole: a possible mechanism for deep earthquake, *J. geophys. Res.,* **75,** 4957–4963.

Minson, S.E., Dreger, D.S., Burgmann, R., Kanamori, H. & Larson, K.M., 2007. Seismically and geodetically determined non-double-couple source mechanisms from the 2000 Miyakejima volcanic earthquake swarm, *J. geophys. Res.,* **112,** B10308, doi:10.1029/2006JB004847.

Patton, H.J. & Taylor, S.R., 2011. The apparent explosion moment: inferences of volumetric moment due to source medium damage by underground nuclear explosions, *J. geophys. Res.,* **116,** B3, doi:10.1029/2010JB007937.

Pondrelli, S., Salimbeni, S., Ekstrom, G., Morelli, A., Gasperini, P. & Vannucci, G., 2006. The Italian CMT dataset from 1977 to the present, *Phys. Earth planet. Inter.,* **159,** 286–303.

Riedesel, M.A. & Jordan, T.H., 1989. Display and assessment of seismic moment tensors, *Bull. seism. Soc. Am.,* **79,** 85–100.

Ritsema, J. & Lay, T., 1993. Rapid source mechanism determination of large ($M_w \geq 5$) earthquakes in the western United States, *Geophys. Res. Lett.,* **20,** 1611–1614.

Tape, W. & Tape, C., 2012a. A geometric setting for moment tensors, *Geophys. J. Int.,* **190,** 476–498.

Tape, W. & Tape, C., 2012b. A geometric comparison of source-type plots for moment tensors, *Geophys. J. Int.,* **190,** 499–510.

Walter, F., Clinton, J.F., Deichmann, N., Dreger, D.S., Minson, S.E. & Funk, M., 2009. Moment tensor inversions of icequakes on Gornergletscher, Switzerland, *Bull. seism. Soc. Am.,* **99,** 852–870.

Zhao, L.S. & Helmberger, D.V., 1994. Source estimation from broadband regional seismograms, *Bull. seism. Soc. Am.,* **84,** 91–104.

Zhu, L. & Helmberger, D.V., 1996. Advancement in source estimation techniques using broadband regional seismograms, *Bull. seism. Soc. Am.,* **86,** 1634–1641.